Crystal Structure of $[(C_2H_5)_4N]_3[Fe_4S_4(SCH_2Ph)_4]$, a Reduced Ferredoxin Site Analogue with a Nontetragonal Fe_4S_4 Core Structure in the Solid State

Jeremy M. Berg, Keith O. Hodgson,[1] and R. H. Holm*

Contribution from the Department of Chemistry, Stanford University, Stanford, California 94305. *Received December 12, 1978*

Abstract: Determination of the structure of the title compound, a synthetic analogue of the 4-Fe sites of reduced ferredoxin (Fd) proteins, was undertaken in order to clarify the source of substantial differences in ^{57}Fe Mössbauer spectral and magnetic properties between it and those of the isoelectronic trianion $[Fe_4S_4(SPh)_4]^{3-}$ in the solid state. $(Et_4N)_3[Fe_4S_4(SCH_2Ph)_4]$ crystallizes in the monoclinic space group *Cc* with 4 formula units in a cell of dimensions $a = 30.318$ (11) Å, $b = 11.469$ (2) Å, $c = 21.412$ (7) Å, and $\beta = 123.25$ (2)°. Using 3482 unique data with $F_o^2 > 3\sigma(F_o^2)$ the structure was refined to $R = 4.3\%$. In contrast to the $[Fe_4S_4*]^+$ core structure of the Fd_{red} site analogue $[Fe_4S_4(SPh)_4]^{3-}$, which is distorted from cubic toward an elongated D_{2d} geometry (eight short + four long Fe-S* bonds), the core of $[Fe_4S_4(SCH_2Ph)_4]^{3-}$ contains six short (mean 2.302 (4) Å) and six long (mean 2.331 (4) Å) Fe-S* bonds so arranged to afford idealized C_{2v} symmetry. Inasmuch as the Fd_{ox} analogues $[Fe_4S_4(SR)_4]^{2-}$ exhibit a highly uniform compressed D_{2d} core geometry (four short + eight long Fe-S* bonds), $[Fe_4S_4(SCH_2Ph)_4]^{3-}$ is the only site analogue yet shown by diffraction methods to possess a nontetragonal core stereochemistry. Brief dianion-trianion and trianion-trianion structural comparisons are presented. The small core structural differences between the two trianions are considered the most likely source of the differences in physicochemical properties in the solid state. A previous investigation has shown that these properties become essentially coincident when the two trianions are examined in frozen and fluid acetonitrile solutions. It is therefore concluded that the unconstrained core structural change accompanying the $[Fe_4S_4(SR)_4]^{2-,3-}$ electron transfer reaction is compressed $D_{2d} \leftrightarrow$ elongated D_{2d} rather than compressed $D_{2d} \leftrightarrow C_{2v}$, and that the less symmetric core structure of $[Fe_4S_4(SCH_2Ph)_4]^{3-}$ in its crystalline tetraethylammonium salt is the consequence of solid state environmental factors.

Introduction

As part of the research program whose goal is the development of synthetic analogues[2] of the redox sites of iron-sulfur proteins[3] in all physiologically significant oxidation levels, the tetranuclear trianions $[Fe_4S_4(SR)_4]^{3-}$ (R = CH_2Ph, aryl) have recently been synthesized[4,5] and certain of their electronic properties examined in detail.[5-7] These investigations have established the isoelectronic relationship $[Fe_4S_4(SR)_4]^{3-} \equiv Fd_{red}$ between synthetic trianions and the 4-Fe sites of reduced ferredoxin proteins. The relationship $[Fe_4S_4(SR)_4]^{2-} \equiv Fd_{ox}$, HP_{red} (HP is a "high-potential" Fe-S protein) has been amply demonstrated previously.[2] In the latter case the analogue-protein site relationship extends to details of structure. Thus the species $[Fe_4S_4(SCH_2Ph)_4]^{2-}$,[8] $[Fe_4S_4(SPh)_4]^{2-}$,[9] $[Fe_4S_4(SCH_2CH_2CO_2)_4]^{6-}$,[10] and $[Fe_4S_4Cl_4]^{2-}$[11] contain $[Fe_4S_4*]^{2+}$ cores which are distorted from idealized T_d-$\bar{4}3m$ symmetry toward D_{2d}-$\bar{4}2m$ symmetry and are structurally closely related to the core units in *Peptococcus aerogenes* Fd_{ox}[12,13] and *Chromatium* HP_{red}.[13] The form of the major distortion is *compression* along the idealized $\bar{4}$ axis such that Fe-S* distances divide into the sets four short + eight long differing by 0.03-0.07 Å. Two such structures are illustrated in Figure 1. The striking uniformity of this core structure (which is also found for the $[Fe_4Se_4]^{2+}$ core of $[Fe_4Se_4(SPh)_4]^{2-}$[14]) indicates that it is not significantly influenced by crystal packing nor, apparently, by protein structure; therefore, it is considered to be the intrinsically stable configuration of this oxidation level.

In contrast to the foregoing cluster species the structure of $[Fe_4S_4(SPh)_4]^{3-}$ in its Et_3MeN^+ salt was found to contain two independent anions whose $[Fe_4S_4*]^+$ cores, although distorted toward D_{2d} symmetry, are *elongated* along their idealized $\bar{4}$ axes.[7] In this case Fe-S* distances divide into the sets four long + eight short differing by ca. 0.07 Å (Figure 1). No Fd_{red} structures are available for comparison. The magnetic and ^{57}Fe Mössbauer spectral data summarized in Table I have structural implications. It was recently concluded from comparison of these data that $[Fe_4S_4(SPh)_4]^{3-}$ has essentially the same structure in the solid and solution states, and that $[Fe_4S_4(SCH_2Ph)_4]^{3-}$ has the elongated D_{2d} structure in acetonitrile solution but not in its crystalline Et_4N^+ salt.[7] Thus the structures of the reduced clusters $[Fe_4S_4(SR)_4]^{3-}$ may be much more sensitive to environmental factors than those of $[Fe_4S_4(SR)_4]^{2-}$. Here we report the detailed structure of $(Et_4N)_3[Fe_4S_4(SCH_2Ph)_4]$, which is found to possess the only nontetragonal Fe_4S_4* core geometry thus far observed for synthetic analogues of protein sites.

Experimental Section

$(Et_4N)_3[Fe_4S_4(SCH_2Ph)_4]$. This compound was synthesized by the procedure of Cambray et al.[4] Suitable single crystals were obtained by slow recrystallization from acetonitrile-THF as described for $(Et_3MeN)_3[Fe_4S_4(SPh)_4]$.[7]

Crystal Data for $(Et_4N)_3[Fe_4S_4(SCH_2Ph)_4]$. X-ray diffraction studies were performed on a Syntex $P2_1$ four-circle diffractometer using graphite-monochromatized Mo $K\bar{\alpha}$ radiation. Air-sensitive black crystals were mounted in glass capillaries under a dinitrogen atmosphere. The crystal system and unit cell dimensions (Table II) were determined from 15 machine-centered reflections selected from a rotation photograph. Partial rotation photographs around the axes confirmed the $2/m$ diffraction symmetry of the monoclinic crystal system. A short data set was collected ($1° < 2\theta < 15°$) from which the following systematic absences were observed: (hkl, $h + k = 2n$ present, $h0l$, $l = 2n$ present). Two space groups, *Cc* and $C2/c$, are consistent with these conditions. Based on the observed density of 1.29 g/cm^3, which was determined by flotation in $CHBr_3$ and hexane, four units each consisting of one anion and three cations would be present per unit cell. Since *Cc* gives $Z = 4$ in the general position while $C2/c$ gives $Z = 8$, the space group was tentatively assigned to be *Cc*. Subsequent solution and refinement of the structure confirmed *Cc* as the correct choice. Final lattice parameters and the orientation matrix were determined by least-squares refinement of 15 reflections chosen from the short data set. Crystal data are summarized in Table II.

Data Collection and Reduction. The crystal selected for data collection gave ω scans for several low-angle reflections with full widths at half height of <0.25°. The data collection parameters are given in Table II. Since the space group was presumed to be acentric, a full sphere of data was collected for $2° < 2\theta < 30°$. In addition, $\pm h$, $+k$, $+l$ data were collected for $30° < 2\theta < 41°$. Three standards were

0002-7863/79/1501-4586$01.00/0

Table I. Mössbauer and Magnetic Properties[a] of Tetranuclear Trianions in Crystalline and Solution Phases

		crystalline	
T, K	property	$(Et_3MeN)_3[Fe_4S_4(SPh)_4]$	$(Et_4N)_3[Fe_4S_4(SCH_2Ph)_4]$
4.2	δ_1,[b] $(\Delta E_Q)_1$[b]	0.62, 1.98	0.60, 1.41
	δ_2, $(\Delta E_Q)_2$	0.58, 1.10	0.60, 0.93
4.2	μ_t[c]	2.03	3.35
100		3.37	3.92
299		4.56	5.13

		CH_3CN solution	
T, K	property	$[Fe_4S_4(SPh)_4]^{3-}$	$[Fe_4S_4(SCH_2Ph)_4]^{3-}$
4.2	δ_1, $(\Delta E_Q)_1$	0.63, 2.01	0.64, 2.01
	δ_2, $(\Delta E_Q)_2$	0.57, 1.11	0.59, 1.12
230	μ_t[d]	3.22	3.30
304		3.70	3.77

[a] Data from ref 7 unless otherwise noted. [b] mm/s. [c] μ_B. [d] Reference 5.

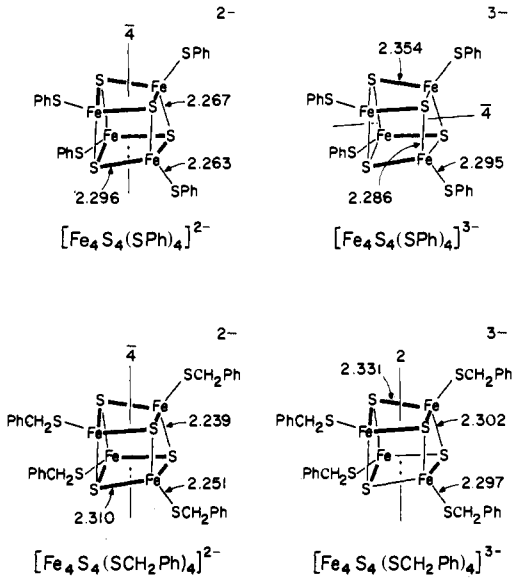

Figure 1. Schematic structures of $[Fe_4S_4^*(SR)_4]^{2-,3-}$ complexes presented in orientations of maximum congruence of the two dianion $Fe_4S_4^*$ cores and of dianion and trianion cores of complexes with the same R group. Idealized symmetry axes and mean values of Fe-S and sets of longer (dark lines) and shorter Fe-S* bonds are shown. Cores of the two trianions can be brought into maximum congruence by a 90° counterclockwise rotation of the mirror image of the $[Fe_4S_4(SPh)_4]^{3-}$ structure about an axis normal to the $\bar{4}$ axis and passing through the top and bottom $Fe_2S_2^*$ core faces (see also footnote 22).

Table II. Summary of Crystal Data, Intensity Collection, and Structure Refinement of $(Et_4N)_3[Fe_4S_4(SCH_2Ph)_4]$

formula	$C_{52}H_{88}Fe_4N_3S_8$
a, Å	30.318 (11)
b, Å	11.469 (2)
c, Å	21.412 (7)
β, deg	123.25 (2)
crystal system	monoclinic
V, Å^3	6227 (7)
Z	4
d_{calcd}, g/cm^3	1.32
d_{obsd}, g/cm^3 [a]	1.29
space group	*Cc*
crystal dimensions,[b] mm	0.30 × 0.35 × 0.40
crystal faces	(100), ($\bar{3}$01), (30$\bar{4}$), ($\bar{3}$1$\bar{1}$), (310)
radiation[c]	Mo(λ K$\bar{\alpha}$ 0.710 69 Å)
absorption coefficient, μ, cm^{-1}	12.3
transmission factors, %	70.24 min, 91.78 max, 79.03 av
takeoff angle, deg	3.0
scan speed, deg/min	1.5 to 29.3 ($\theta/2\theta$ scan)
scan range, deg	0.65 below Kα_1 to 0.65 above Kα_2
background/scan time ratio	0.25
data collected	2θ of 2-30° $\pm h$, $\pm k$, $\pm l$ 2θ of 30-41° $\pm h$, $+k$, $+l$
unique averaged data including Friedel pairs ($F_o^2 > 3\sigma(F_o)^2$)	3482
no. of variables	542
error in observation of unit weight	1.25
R, %	4.3
R_w, %	4.6

[a] Determined by flotation in $CHBr_3$ and hexane. [b] Irregularly shaped crystal. [c] Mosaic graphite monochromator.

collected every 60 reflections. Their intensities showed a 10% decrease over the data collection. Because of this behavior an anisotropic decay correction was applied to the data based on these standards.[15]

The processing of the data was performed as described previously.[11] An analytical absorption correction was applied to the complete data set. At this point the equivalent data which reflect the true *m* diffraction symmetry were averaged. This resulted in 3482 reflections with $F^2 > 3\sigma(F^2)$ including the Friedel pairs which were collected. This data set was used for the final refinement of the structure.

Structure Solution and Refinement. The structure was solved using the direct methods program MULTAN. Trial coordinates for the four Fe and eight S atoms were generated and refined by least squares. The coordinates of the C and N atoms were determined from subsequent difference Fourier maps. Isotropic full-matrix least-squares refinement of all the nonhydrogen coordinates, using statistical weighting as described previously,[11,15] gave R_w = 8.1%. Inversion of this set of coordinates generated the enantiomorph which refined to R_w = 7.9%. Inspection of individual Friedel pairs confirmed that the second choice of coordinates was correct. Anisotropic refinement included all nonhydrogen atoms in the anion and the nitrogen and methyl group carbon atoms in the cations. After these refinements had converged, hydrogen atom positions were calculated assuming trigonal geometries for the phenyl ring hydrogens and tetrahedral geometries for the hydrogen atoms on the cations. Staggered conformations for the methyl hydrogens were assumed. The C-H distance was taken as 0.98 Å and the temperature factors were set to values comparable to those of the carbon atoms to which they are bonded. Fixed contributions from these hydrogens were included in the final refinement cycles. The final refinement cycle converged to R = 4.3%, R_w = 4.6%. The final error in an observation of unit weight was 1.25 electrons. A final difference Fourier map showed no peaks greater than 25% of the height of a carbon atom peak.

The following results for $(Et_4N)_3[Fe_4S_4(SCH_2Ph)_4]$ are tabulated: positional and thermal parameters (Table III); distances and angles in the anion (Table IV); best weighted least-squares planes of the $Fe_4S_4^*$ core of the anion and atomic deviations therefrom (Table V); root mean square amplitudes of thermal vibrations ($Fe_4S_4(SC)_4$ group only, Table VI); values of F_o^2 and F_c^2 (Table VII[16]); calculated hy-

Table III. Positional and Thermal Parameters for $(Et_4N)_3[Fe_4S_4(SCH_2Ph)_4]$

atom	x	y	z	β_{11}[a]	β_{22}	β_{33}	β_{12}	β_{13}	β_{23}
				Anion					
Fe(1)	0.820 31 (0)[b]	0.7570 (1)	0.630 86 (0)	0.001 49 (2)	0.0078 (1)	0.003 01 (4)	0.0005 (1)	0.001 93 (4)	0.0001 (2)
Fe(2)	0.774 06 (5)	0.7502 (1)	0.711 84 (8)	0.001 92 (2)	0.0053 (1)	0.003 47 (4)	−0.0001 (1)	0.003 09 (4)	−0.0004 (1)
Fe(3)	0.849 16 (6)	0.9177 (1)	0.740 08 (8)	0.001 66 (2)	0.0063 (1)	0.003 39 (5)	−0.0010 (1)	0.001 87 (5)	0.0001 (2)
Fe(4)	0.749 98 (5)	0.9278 (1)	0.609 32 (8)	0.001 79 (2)	0.0057 (1)	0.003 43 (4)	0.0000 (1)	0.002 26 (4)	0.0003 (2)
S(1)	0.770 63 (10)	0.9494 (2)	0.7309 (1)	0.002 26 (4)	0.0058 (3)	0.004 50 (9)	−0.0002 (2)	0.003 79 (9)	−0.0012 (3)
S(2)	0.828 88 (10)	0.9541 (3)	0.6199 (1)	0.002 14 (5)	0.0091 (3)	0.003 35 (9)	−0.0009 (2)	0.002 77 (9)	0.0030 (3)
S(3)	0.732 19 (9)	0.7295 (2)	0.5834 (1)	0.001 53 (4)	0.0067 (3)	0.004 15 (9)	−0.0004 (2)	0.002 65 (8)	−0.0016 (3)
S(4)	0.861 74 (10)	0.7192 (2)	0.7578 (1)	0.001 53 (4)	0.0071 (3)	0.002 28 (8)	0.0008 (2)	0.000 95 (8)	0.0009 (3)
S(5)	0.854 87 (11)	0.6436 (3)	0.5788 (2)	0.002 18 (5)	0.0123 (4)	0.004 76 (10)	−0.0004 (2)	0.003 97 (9)	−0.0024 (3)
S(6)	0.738 50 (11)	0.6319 (3)	0.7588 (2)	0.002 01 (5)	0.0098 (3)	0.005 00 (10)	−0.0005 (2)	0.003 77 (9)	0.0039 (3)
S(7)	0.922 77 (12)	1.0226 (3)	0.8244 (2)	0.002 27 (6)	0.0100 (3)	0.005 11 (12)	−0.0024 (2)	0.002 07 (12)	−0.0022 (4)
S(8)	0.690 68 (11)	1.0590 (3)	0.5216 (2)	0.001 91 (5)	0.0084 (3)	0.004 55 (11)	0.0013 (2)	0.001 47 (11)	0.0022 (3)
C(1)	0.9232 (4)	0.693 (1)	0.6391 (7)	0.0015 (2)	0.018 (1)	0.0095 (5)	−0.0045 (9)	0.0045 (4)	−0.020 (1)
C(2)	0.6712 (5)	0.679 (1)	0.7120 (8)	0.0042 (3)	0.011 (2)	0.0129 (7)	0.0003 (11)	0.0098 (5)	−0.001 (2)
C(3)	0.9674 (5)	0.992 (1)	0.7929 (7)	0.0028 (2)	0.020 (2)	0.0099 (6)	−0.0001 (12)	0.0053 (5)	−0.012 (2)
C(4)	0.6382 (4)	1.065 (1)	0.5390 (7)	0.0030 (2)	0.014 (1)	0.0082 (5)	0.0038 (10)	0.052 (5)	−0.004 (1)
R(1)C(1)[d]	0.9607 (4)	0.623 (1)	0.6316 (6)	0.0021 (2)	0.010 (1)	0.0092 (5)	−0.0051 (8)	0.0060 (4)	−0.012 (1)
R(1)C(2)	0.9887 (4)	0.527 (1)	0.6709 (7)	0.0027 (2)	0.014 (2)	0.0099 (6)	−0.0074 (10)	0.0049 (5)	−0.006 (2)
R(1)C(3)	1.0267 (5)	0.469 (2)	0.6632 (8)	0.0016 (2)	0.033 (2)	0.0134 (7)	0.0024 (12)	0.0024 (6)	−0.026 (2)
R(1)C(4)	1.0262 (5)	0.509 (2)	0.6007 (9)	0.0021 (3)	0.030 (2)	0.0128 (8)	0.0005 (13)	0.0026 (7)	−0.023 (2)
R(1)C(5)	0.9995 (5)	0.596 (2)	0.5593 (7)	0.0050 (2)	0.030 (3)	0.0147 (5)	−0.0080 (13)	0.0148 (4)	−0.015 (2)
R(1)C(6)	0.9699 (5)	0.652 (1)	0.5751 (8)	0.0039 (3)	0.021 (2)	0.0105 (6)	−0.0032 (12)	0.0089 (5)	−0.009 (2)
R(2)C(1)	0.6308 (4)	0.586 (1)	0.6802 (7)	0.0024 (2)	0.015 (2)	0.0094 (5)	0.0022 (10)	0.0063 (4)	0.006 (2)
R(2)C(2)	0.6016 (4)	0.576 (1)	0.7108 (7)	0.0023 (2)	0.017 (2)	0.0098 (6)	0.0046 (11)	0.0054 (5)	0.007 (2)
R(2)C(3)	0.5659 (6)	0.487 (2)	0.6889 (9)	0.0033 (4)	0.033 (3)	0.0108 (8)	0.0000 (18)	0.0038 (8)	0.014 (3)
R(2)C(4)	0.5561 (6)	0.426 (2)	0.6238 (13)	0.0014 (3)	0.033 (3)	0.0207 (15)	−0.0092 (15)	−0.0082 (11)	0.023 (3)
R(2)C(5)	0.5840 (8)	0.439 (2)	0.6014 (13)	0.0048 (5)	0.019 (2)	0.0177 (15)	−0.0044 (19)	−0.0042 (15)	−0.009 (3)
R(2)C(6)	0.6194 (5)	0.518 (1)	0.6229 (7)	0.0039 (3)	0.030 (2)	0.0075 (6)	0.0094 (13)	0.0037 (6)	−0.007 (2)
R(3)C(1)	1.0154 (4)	1.061 (1)	0.8268 (7)	0.0016 (2)	0.015 (2)	0.0073 (5)	−0.0030 (10)	0.0026 (5)	0.001 (2)
R(3)C(2)	1.0236 (6)	1.161 (1)	0.8057 (9)	0.0037 (3)	0.014 (2)	0.0137 (9)	0.0000 (13)	0.0061 (8)	0.010 (2)
R(3)C(3)	1.0706 (7)	1.224 (1)	0.8404 (10)	0.0080 (4)	0.010 (2)	0.0147 (8)	−0.0039 (14)	0.0129 (8)	0.003 (2)
R(3)C(4)	1.1045 (5)	1.177 (1)	0.8993 (8)	0.0054 (3)	0.013 (2)	0.0145 (7)	−0.0100 (11)	0.0122 (6)	−0.010 (2)
R(3)C(5)	1.1060 (5)	1.082 (2)	0.9273 (8)	0.0020 (3)	0.039 (3)	0.0068 (6)	−0.0070 (15)	0.0020 (6)	−0.007 (2)
R(3)C(6)	1.0589 (5)	1.011 (1)	0.8904 (7)	0.0039 (2)	0.021 (2)	0.0089 (5)	0.0013 (12)	0.0085 (5)	−0.001 (2)
R(4)C(1)	0.5905 (3)	0.985 (1)	0.4895 (5)	0.0015 (2)	0.022 (2)	0.0033 (4)	0.0086 (8)	0.0021 (3)	0.004 (1)
R(4)C(2)	0.5455 (4)	1.019 (2)	0.4301 (6)	0.0020 (2)	0.035 (3)	0.0058 (5)	0.0042 (13)	0.0040 (4)	0.009 (2)
R(4)C(3)	0.5032 (5)	0.943 (2)	0.3865 (7)	0.0026 (3)	0.035 (3)	0.0043 (5)	−0.0007 (16)	0.0013 (5)	0.010 (2)
R(4)C(4)	0.5125 (5)	0.835 (2)	0.4102 (6)	0.0029 (2)	0.041 (3)	0.0040 (4)	−0.0036 (14)	0.0039 (4)	−0.007 (2)
R(4)C(5)	0.5594 (5)	0.794 (2)	0.4722 (8)	0.0025 (2)	0.031 (3)	0.0066 (5)	−0.0021 (14)	0.0035 (5)	0.000 (2)
R(4)C(6)	0.5998 (4)	0.869 (1)	0.5111 (7)	0.0021 (2)	0.022 (2)	0.0066 (5)	0.0058 (10)	0.0034 (4)	−0.006 (2)
				Cations[a]					
N(1)	0.8859 (3)	0.8047 (7)	0.9872 (4)	0.0029 (2)	0.0086 (9)	0.0025 (3)	0.0000 (7)	0.0025 (3)	−0.0002 (9)
N(2)	0.8130 (4)	0.3395 (6)	0.7007 (4)	0.0037 (2)	0.0048 (8)	0.0059 (3)	−0.0001 (7)	0.0062 (3)	−0.0017 (8)
N(3)	0.6787 (3)	0.7972 (9)	0.3501 (4)	0.0018 (1)	0.0180 (12)	0.0047 (3)	0.0011 (7)	0.0024 (3)	0.0098 (10)
C(9)	0.7898 (5)	0.824 (1)	0.9418 (9)	0.0022 (3)	0.020 (2)	0.0094 (8)	0.003 (1)	−0.0004 (8)	0.003 (2)
C(10)	0.9823 (5)	0.791 (1)	1.0351 (8)	0.0044 (3)	0.023 (2)	0.0123 (6)	−0.004 (1)	0.0095 (6)	−0.015 (2)
C(11)	0.9046 (7)	1.025 (1)	1.0054 (13)	0.0039 (4)	0.015 (2)	0.0272 (15)	−0.005 (2)	0.0073 (12)	−0.026 (3)
C(12)	0.8699 (6)	0.592 (1)	0.9604 (9)	0.0048 (3)	0.016 (2)	0.0142 (7)	0.008 (1)	0.0093 (7)	0.021 (2)
C(17)	0.8694 (5)	0.321 (1)	0.8415 (7)	0.0059 (3)	0.016 (2)	0.0064 (5)	0.006 (1)	0.0076 (5)	0.001 (2)
C(18)	0.8995 (6)	0.363 (1)	0.7065 (8)	0.0041 (3)	0.019 (2)	0.0080 (6)	0.006 (1)	0.0048 (6)	−0.004 (2)
C(19)	0.7599 (6)	0.402 (1)	0.5642 (7)	0.0048 (4)	0.008 (1)	0.0050 (5)	−0.003 (1)	0.0011 (7)	0.004 (1)
C(20)	0.7236 (5)	0.292 (1)	0.6783 (6)	0.0062 (2)	0.020 (2)	0.0087 (4)	−0.012 (1)	0.0120 (4)	−0.010 (1)
C(25)	0.7765 (5)	0.836 (1)	0.4060 (7)	0.0031 (3)	0.016 (2)	0.0044 (6)	−0.003 (1)	−0.0031 (8)	0.006 (2)
C(26)	0.5908 (5)	0.765 (1)	0.3226 (7)	0.0048 (3)	0.019 (2)	0.0068 (5)	0.003 (1)	0.0075 (5)	0.004 (2)
C(27)	0.7059 (5)	0.581 (1)	0.3869 (7)	0.0038 (3)	0.008 (1)	0.0058 (5)	0.003 (1)	0.0017 (6)	0.004 (1)
C(28)	0.6598 (6)	1.001 (2)	0.2965 (9)	0.0032 (4)	0.023 (2)	0.0094 (8)	−0.004 (2)	0.0002 (9)	0.009 (2)
		B (Å^2)							
C(5)	0.8451 (6)	0.8182 (15)	1.0078 (8)	11.9 (5)					
C(6)	0.9368 (6)	0.8041 (16)	1.0596 (9)	12.7 (6)					
C(7)	0.8843 (6)	0.9189 (16)	0.9449 (9)	13.1 (6)					
C(8)	0.8711 (6)	0.7100 (18)	0.9360 (9)	14.5 (6)					
C(13)	0.8355 (4)	0.3988 (11)	0.7764 (6)	6.6 (3)					
C(14)	0.8557 (4)	0.2801 (10)	0.6906 (5)	5.6 (3)					
C(15)	0.7878 (4)	0.4371 (9)	0.6430 (5)	5.3 (3)					
C(16)	0.7762 (4)	0.2451 (10)	0.6869 (6)	6.3 (3)					
C(21)	0.7348 (4)	0.8294 (12)	0.4170 (6)	7.8 (4)					
C(22)	0.6450 (4)	0.8054 (11)	0.3784 (6)	6.4 (3)					
C(23)	0.6853 (4)	0.6726 (11)	0.3252 (6)	6.8 (3)					
C(24)	0.6658 (5)	0.8783 (12)	0.2845 (7)	8.9 (4)					

[a] The form of the anisotropic thermal ellipsoid is $\exp[-(\beta_{11}h^2 + \beta_{22}k^2 + \beta_{33}l^2 + \beta_{12}hk + \beta_{13}hl + \beta_{23}kl)]$. [b] Estimated standard deviations in parentheses in this and succeeding tables. [c] Rings numbered according to carbon atoms (C(1)-C(4)) to which they are attached. [d] Numbering scheme: N(1), C(5)-C(12); N(2), C(13)-C(20); N(3), C(21)-C(28).

drogen atom positions (cations and anion, Table VIII[16]); comparison of structural parameters of $[Fe_4S_4(SCH_2Ph)_4]^{2-,3-}$ and $[Fe_4S_4(SPh)_4]^{3-}$ (Table IX).

Core Congruence. Stereochemical relationships between Fe_4S_4* cores and their Fe_4 subunits in different $[Fe_4S_4(SR)_4]^{2-,3-}$ structures (R = Ph, CH_2Ph) were investigated as described previously.[7] A computer program[17] calculated the quantity Q in eq 1 for convergent refinement of each of the 12 possible relative orientations of two cores or Fe_4 subunits (A, B), whose atomic coordinates are available from this work (Table III) and prior investigations.[7-9] Here n is the number of atoms and σ is the estimated standard deviation in coordinate $q^i = x, y, z$. Maximum congruence of reference object (fixed spatial orientation) and image (variable spatial orientation) was decided using the least-squares criterion that the quantity Q be minimized. The

Table IV. Selected Distances (Å) and Angles (deg) in $[Fe_4S_4(SCH_2Ph)_4]^{3-}$

Fe-S		Fe-S*	
Fe(1)-S(5)	2.304 (6)	Fe(1)-S(2)	2.302 (5)
Fe(2)-S(6)	2.281 (5)	Fe(1)-S(3)	2.300 (5)
Fe(3)-S(7)	2.296 (5)	Fe(2)-S(4)	2.301 (5)
Fe(4)-S(8)	2.307 (5)	Fe(3)-S(1)	2.308 (5)
mean	2.297 (12)	Fe(3)-S(4)	2.306 (5)
		Fe(4)-S(2)	2.296 (5)
Fe···S*		mean	2.302 (4)
Fe(1)-S(1)	3.908 (5)	Fe(1)-S(4)	2.327 (5)
Fe(2)-S(2)	3.962 (5)	Fe(2)-S(1)	2.333 (5)
Fe(3)-S(3)	3.931 (5)	Fe(2)-S(3)	2.325 (5)
Fe(4)-S(4)	3.937 (5)	Fe(3)-S(2)	2.333 (5)
mean	3.935 (22)	Fe(4)-S(1)	2.334 (5)
		Fe(4)-S(3)	2.332 (5)
Fe···Fe		mean	2.331 (4)
Fe(1)-Fe(2)	2.765 (2)	mean of 12	2.316 (15)
Fe(1)-Fe(3)	2.719 (3)		
Fe(1)-Fe(4)	2.742 (3)	S*···S*	
Fe(2)-Fe(3)	2.780 (3)	S(1)-S(2)	3.658 (4)
Fe(2)-Fe(4)	2.782 (3)	S(1)-S(4)	3.631 (6)
Fe(3)-Fe(4)	2.768 (2)	S(2)-S(3)	3.650 (3)
mean	2.759 (24)	S(3)-S(4)	3.648 (3)
		mean	3.647 (11)
		S(1)-S(3)	3.696 (6)
		S(2)-S(4)	3.708 (6)
		mean	3.702
		mean of 6	3.665 (30)
Fe-S*-Fe		S-Fe-S*	
Fe(2)-S(1)-Fe(3)	73.62 (15)	S(5)-Fe(1)-S(2)	113.44 (21)
Fe(2)-S(1)-Fe(4)	73.19 (16)	S(5)-Fe(1)-S(3)	115.78 (20)
Fe(3)-S(1)-Fe(4)	73.22 (16)	S(5)-Fe(1)-S(4)	111.27 (19)
Fe(1)-S(2)-Fe(3)	71.83 (15)	S(6)-Fe(2)-S(1)	115.35 (21)
Fe(1)-S(2)-Fe(4)	73.21 (16)	S(6)-Fe(2)-S(3)	112.16 (20)
Fe(3)-S(2)-Fe(4)	73.45 (16)	S(6)-Fe(2)-S(4)	115.70 (20)
Fe(1)-S(3)-Fe(2)	73.41 (15)	S(7)-Fe(3)-S(1)	119.81 (21)
Fe(1)-S(3)-Fe(4)	72.58 (15)	S(7)-Fe(3)-S(2)	109.21 (20)
Fe(2)-S(3)-Fe(4)	73.36 (15)	S(7)-Fe(3)-S(4)	112.71 (19)
Fe(1)-S(4)-Fe(2)	73.38 (14)	S(8)-Fe(4)-S(1)	116.85 (19)
Fe(1)-S(4)-Fe(3)	71.88 (15)	S(8)-Fe(4)-S(2)	107.41 (19)
Fe(2)-S(4)-Fe(3)	74.26 (16)	S(8)-Fe(4)-S(3)	117.83 (18)
mean	73.12[a]	mean	113.96
Fe-Fe-Fe		S*-S*-S*	
Fe(2)-Fe(1)-Fe(3)	60.93 (9)	S(2)-S(1)-S(3)	59.51 (12)
Fe(2)-Fe(1)-Fe(4)	60.69 (9)	S(2)-S(1)-S(4)	61.15 (13)
Fe(3)-Fe(1)-Fe(4)	60.92 (7)	S(3)-S(1)-S(4)	59.71 (9)
Fe(1)-Fe(2)-Fe(3)	58.72 (9)	S(1)-S(2)-S(3)	60.76 (12)
Fe(1)-Fe(2)-Fe(4)	59.25 (9)	S(1)-S(2)-S(4)	59.07 (13)
Fe(3)-Fe(2)-Fe(4)	59.69 (7)	S(3)-S(2)-S(4)	59.44 (10)
Fe(1)-Fe(3)-Fe(2)	60.35 (7)	S(1)-S(3)-S(2)	59.72 (9)
Fe(1)-Fe(3)-Fe(4)	59.96 (9)	S(1)-S(3)-S(4)	59.26 (12)
Fe(2)-Fe(3)-Fe(4)	60.18 (9)	S(2)-S(3)-S(4)	61.06 (12)
Fe(1)-Fe(4)-Fe(2)	60.06 (7)	S(1)-S(4)-S(2)	59.79 (9)
Fe(1)-Fe(4)-Fe(3)	59.13 (9)	S(1)-S(4)-S(3)	61.03 (12)
Fe(2)-Fe(4)-Fe(3)	60.13 (9)	S(2)-S(4)-S(3)	59.50 (12)
mean	60.00	mean	60.00
S*-Fe-S*		C-C (ring)	
S(2)-Fe(1)-S(3)	104.95 (20)	C(1)-R(1)C(1)	1.471 (25)
S(2)-Fe(1)-S(4)	106.45 (18)	C(2)-R(2)C(1)	1.480 (29)
S(3)-Fe(1)-S(4)	104.08 (22)	C(3)-R(3)C(1)	1.456 (22)
S(1)-Fe(2)-S(3)	105.05 (19)	C(4)-R(4)C(1)	1.542 (23)
S(1)-Fe(2)-S(4)	103.20 (19)	mean	1.487
S(3)-Fe(2)-S(4)	104.12 (21)		
S(1)-Fe(3)-S(2)	104.05 (20)	S-C-C (ring)	
S(1)-Fe(3)-S(4)	103.82 (19)	S(5)-C(1)-R(1)C(1)	113.41
S(2)-Fe(3)-S(4)	106.14 (19)	S(6)-C(2)-R(2)C(1)	116.13
S(1)-Fe(4)-S(2)	104.38 (19)	S(7)-C(3)-R(3)C(1)	116.54
S(1)-Fe(4)-S(3)	104.77 (19)	S(8)-C(4)-R(4)C(1)	115.43
S(2)-Fe(4)-S(3)	104.11 (19)	mean	115.38
mean	104.59		
S-C			
S(5)-C(1)	1.829 (17)		
S(6)-C(2)	1.794 (23)		
S(7)-C(3)	1.848 (19)		
S(8)-C(4)	1.824 (19)		
mean	1.824 (22)		

[a] The standard deviation of the mean was estimated from $\sigma \approx s = [(\Sigma x_i^2 - n\bar{x}^2)/(n-1)]^{1/2}$; no value is given for any angular quantity, as the variations exceed those expected from a sample taken from the same population.

results of these calculations are considered in a following section.

$$Q = \sum_{j=1}^{n} \sum_{i=1}^{3} \frac{(q_A{}^{ij} - q_B{}^{ij})^2}{\sigma^2(q_A{}^{ij}) + \sigma^2(q_B{}^{ij})} \qquad (1)$$

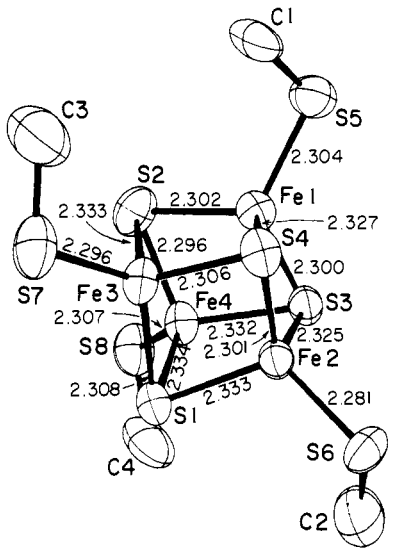

Figure 2. The structure of the $Fe_4S_4(SC)_4$ portion of $[Fe_4S_4(SCH_2Ph)_4]^{3-}$, showing 50% probability ellipsoids, principal interatomic distances, and the atom labeling scheme.

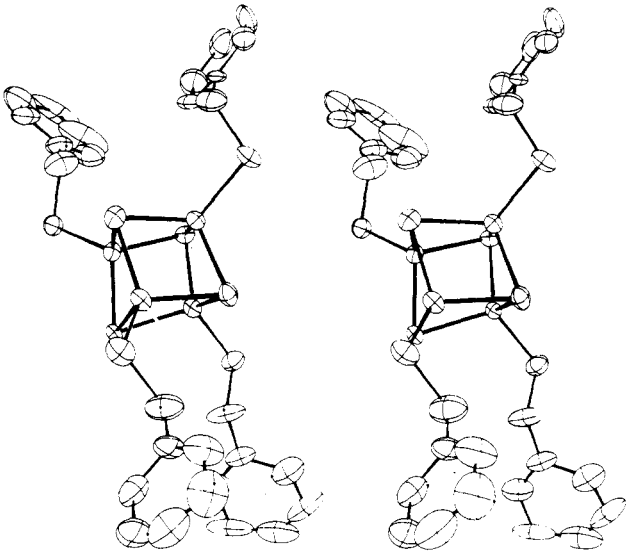

Figure 3. A stereoscopic view of the $[Fe_4S_4(SCH_2Ph)_4]^{3-}$ ion, complete except for hydrogen atoms; 25% probability ellipsoids are shown.

Results and Discussion

Structure of $(Et_4N)_3[Fe_4S_4(SCH_2Ph)_4]$. This compound crystallizes in the monoclinic space group *Cc* and contains three cations and one anion per asymmetric unit. The cations possess the usual tetrahedral geometry, and one exhibits substantial thermal motion as judged from the parameters of Table III. The ranges and mean values of the 12 independent N-C and C-C distances are 1.43 (3)-1.58 (2), 1.52, and 1.41 (2)-1.73 (3), 1.52 Å, respectively. The 18 C-N-C angles vary from 104 (2)° to 121 (2)° and average to 109°.

The structure of a portion of the $[Fe_4S_4(SCH_2Ph)_4]^{3-}$ anion containing the $[Fe_4S_4^*]^+$ core and denoting the atom labeling scheme is shown in Figure 2. A stereoview of the entire anion is presented in Figure 3. Phenyl ring dimensions (not tabulated) are normal and are not further considered. Immediately apparent is the basic cubane-type core stereochemistry observed in the Fd_{ox} and Fd_{red} site analogues $[Fe_4S_4(SR)_4]^{2-}$ (R = CH_2Ph,[8] Ph[9]), $[Fe_4S_4(SCH_2CH_2CO_2)_4]^{6-}$,[10] and $[Fe_4S_4(SPh)_4]^{3-}$,[7] respectively, and in $[Fe_4S_4Cl_4]^{2-}$,[11] $[Fe_4Se_4(SPh)_4]^{2-}$,[14] and other physiologically unrelated M_4S_4 complexes.[18] The following summary of the principal struc-

Table V. Best Weighted Least-Squares Planes for $[Fe_4S_4(SCH_2Ph)_4]^{3-}$

plane no.	$Ax + By + Cz = D$ (orthogonalized coordinates)			
	A	B	C	D
1	−0.5298	0.0330	−0.8475	−18.5374
2	0.8504	0.0055	−0.5261	7.5816
3	0.1602	0.7337	−0.6604	1.7059
4	0.1565	−0.6832	−0.7132	−12.6083
5	−0.6843	0.7174	−0.1308	−5.8457
6	−0.6925	−0.6954	−0.1919	−20.2967
7	0.0229	−0.9982	−0.0553	−8.8619
8	0.2288	0.0276	−0.9731	−8.7852
9	−0.9738	0.0216	−0.2264	−17.3506
10	0.2461	0.0166	−0.9691	−6.4788
11	−0.9785	0.0285	−0.2045	−19.1792
12	−0.0121	−0.9991	−0.0403	−11.3334

atom	deviations, Å, from plane no.					
	1	2	3	4	5	6
Fe(1)	−0.004 (1)		0.001 (1)			−0.003(1)
Fe(2)	0.011 (2)			0.004 (1)	0.009 (2)	
Fe(3)		0.010 (2)	−0.003 (1)		−0.010 (2)	
Fe(4)		−0.009 (2)		−0.004 (1)		0.010 (2)
S(1)	−0.030 (3)		0.007 (3)			−0.025 (3)
S(2)	0.031 (3)			0.010 (3)	0.025 (3)	
S(3)		0.023 (3)	−0.007 (3)		−0.024 (3)	
S(4)		−0.023 (3)		−0.009 (3)		0.024 (3)

atom	7	8	9	10	11	12
Fe(1)	−0.028 (2)			−0.028 (1)	0.023 (1)	
Fe(2)	−0.086 (2)	0.077 (1)	−0.065 (2)			
Fe(3)		0.083 (1)			0.075 (2)	0.077 (1)
Fe(4)			−0.067 (2)	−0.084 (1)		0.075 (1)
S(1)		−0.268 (3)	0.226 (3)			−0.251 (3)
S(2)				0.296 (3)	−0.252 (3)	−0.262 (3)
S(3)	0.284 (3)		0.218 (3)	0.271 (3)		
S(4)	0.273 (3)	−0.249 (2)			−0.225 (3)	

Table VI. Root Mean Square Amplitudes of Thermal Vibration (Å)[a]

atom	min	int	max
Fe(1)	0.212	0.228	0.244
Fe(2)	0.188	0.227	0.250
Fe(3)	0.196	0.225	0.275
Fe(4)	0.194	0.231	0.263
S(1)	0.193	0.258	0.276
S(2)	0.191	0.254	0.296
S(3)	0.205	0.223	0.271
S(4)	0.178	0.221	0.272
S(5)	0.243	0.267	0.304
S(6)	0.202	0.260	0.313
S(7)	0.220	0.288	0.349
S(8)	0.208	0.258	0.338
C(1)	0.174	0.207	0.505
C(2)	0.273	0.335	0.459
C(3)	0.273	0.306	0.479
C(4)	0.224	0.337	0.403

[a] Data for $Fe_4S_4(SC)_4$ atoms only.

tural features of $[Fe_4S_4(SCH_2Ph)_4]^{3-}$ closely follows previous discussions;[7,8,14] attention is directed to the bond distance and angle data in Table IV, atomic displacements from best weighted least-squares planes in Table V, and Figures 1 and 2. (1) The Fe-S* distances of the $[Fe_4S_4*]^{+}$ core divide into sets of six short and six long with mean values of 2.302 (4) and 2.331 (4) Å, respectively, which differ by $\gtrsim 3\sigma$, four of the long distances (Fe(2,4)-S(1,3)) form one polyhedral face with the other two long distances (Fe(3)-S(2), Fe(1)-S(4)) located in the opposite face. (2) The six diagonal planes (1-6) through the core are nearly perfect. (3) Each Fe_2S_2* polyhedral face is a distinctly nonplanar rhomb (planes 7-12, mean S*-Fe-S* and Fe-S*-Fe angles 104.6 and 73.1°, respectively). (4) The Fe_4 and S_4* groups are distorted tetrahedra; in the latter S*···S* distances divide into two long (mean 3.702 Å, located in the faces designated in (1)) and four short (mean 3.647 (11) Å). (5) From (1)-(4) the highest *idealized* symmetry of the core is C_{2v}, with the twofold axis passing through those faces (Fe(1,3)-S(2,4), Fe(2,4)-S(1,3)) containing the long bonds noted in (1); two and four of the short bonds are then approximately perpendicular and parallel, respectively, to this axis. (6) The $Fe_4S_4*S_4$ cluster less closely approaches the idealized core symmetry owing to variations in certain sets of S-Fe-S* angles (total range 107.4-119.8°). (7) The mean value of terminal Fe-S distances exceeds the corresponding value in $[Fe_4S_4(SCH_2Ph)_4]^{2-}$ [8] by 0.046 Å, consistent[19] with higher Fe(II) character in the $[Fe_4S_4]^{+}$ core of the trianion (formally 3Fe(II) + Fe(III)) vs. the $[Fe_4S_4]^{2+}$ core of the dianion (formally 2Fe(II) + 2Fe(III)). (8) Mean values of $S-CH_2$ distances in the dianion (1.832 (3) Å[8]) and trianion (1.824 (22) Å) are within experimental uncertainty of each other, as would be expected for two independent, well-refined structures. Further analysis of the $[Fe_4S_4(SCH_2Ph)_4]^{3-}$ structure is best conducted by the following comparison of related cluster structures in the same and different oxidation levels and concomitant assessment of Fe_4 and core congruencies based on the calculations described in the Experimental Section.

Structural Comparisons. A. Complexes with $[Fe_4S_4]^{2+}$ Cores. As observed at the outset four species with isoelectronic $[Fe_4S_4*]^{2+}$ cores ($[Fe_4S_4(SCH_2Ph)_4]^{2-}$,[8] $[Fe_4S_4(SPh)_4]^{2-}$,[9] $[Fe_4S_4(SCH_2CH_2CO_2)_4]^{6-}$,[10] $[Fe_4S_4Cl_4]^{2-}$[11]) exhibit an essentially constant compressed D_{2d} core geometry. Consequently, these species have a near-degenerate fourfold core

Table IX. Comparison of Mean Values of Selected Structural Parameters for $[Fe_4S_4(SCH_2Ph)_4]^{2-,3-}$ and $[Fe_4S_4(SPh)_4]^{3-}$

property[a]	$[Fe_4S_4*(SCH_2Ph)_4]^{2-}$ [b]	$[Fe_4S_4*(SCH_2Ph)_4]^{3-}$	$[Fe_4S_4*(SPh)_4]^{3-}$ [c]
Fe-S[d]	2.251	2.297	2.295
Fe-S*	2.239 (4), 2.310 (8)[g]	2.302 (6), 2.331 (6)[h]	2.354 (4), 2.286 (8)[l]
Fe···Fe	2.776 (2), 2.732 (4)[i]	2.759	2.743
S*···S*	3.586 (4), 3.645 (2)[j]	3.647 (4), 3.702 (2)	3.592 (2), 3.690 (4)[m]
S-Fe-S*[e]	115.1	114.0	113.6
Fe-S*-Fe	73.8	73.1	72.9
S*-Fe-S*	104.1	104.6	104.8
Fe-Fe-Fe	61.11 (4), 59.46 (8)[k]	60.00	59.98
Fe_4[f]	2.439	2.475	2.432[n]
S_4*	5.519	5.800	5.754
idealized symmetry	D_{2d} (compressed)	C_{2v}	D_{2d} (elongated)

[a] Number of values averaged indicated in parentheses where two distances or angles are given; otherwise, the mean of all values is given. [b] Et_4N^+ salt; data from ref 8. [c] Et_3Me^+ salt; data (anion 1) from ref 7. [d] Distance (Å). [e] Angle (deg). [f] Volume (Å^3). [g-m] Mean of all values. [g] 2.286. [h] 2.316. [i] 2.747. [j] 3.606. [k] 60.01. [l] 2.309. [m] 3.657. [n] Values for $[Fe_4S_4(SPh)_4]^{2-}$: 2.412 (Fe_4), 5.543 (S_4*).

congruency around the idealized 4 axis, approximately parallel to which are the four short Fe-S* distances. Maximally congruent core orientations for two dianions are depicted in Figure 1. Detailed metrical comparisons of isoelectronic complexes and protein sites are available elsewhere.[2,9,10,13,20]

B. $[Fe_4S_4(SPh)_4]^{3-}$ vs. $[Fe_4S_4(SCH_2Ph)_4]^{3-}$. The only previous structural determination of a complex with an $[Fe_4S_4]^+$ core is that of $(Et_3MeN)_3[Fe_4S_4(SPh)_4]$,[7] which contains two crystallographically independent trianions with no significant structural differences between them. The structures of $[Fe_4S_4(SPh)_4]^{3-}$ and $[Fe_4S_4(SCH_2Ph)_4]^{3-}$ are metrically compared in Table IX and schematically in Figure 1. Small core structural differences are evident which are most significant for Fe-S* and S*···S* distances. $[Fe_4S_4(SPh)_4]^{3-}$ has the higher idealized core symmetry (D_{2d}) with the four long Fe-S* bonds parallel to the $\bar{4}$ axis and accounting for the elongated tetragonal geometry; the eight short Fe-S* bonds are roughly perpendicular to this axis. In comparison, the Fe-S* bonds in $[Fe_4S_4(SCH_2Ph)_4]^{3-}$ divide into sets of six long and six short so arranged as to provide idealized C_{2v} core symmetry. Correspondingly, nonbonded S*···S* distances also divide differently. In $[Fe_4S_4(SCH_2Ph)_4]^{3-}$ there are two long distances in faces approximately perpendicular to the twofold axis whereas in $[Fe_4S_4(SPh)_4]^{3-}$ there are four long distances in faces approximately parallel to the $\bar{4}$ axis. Calculations based on eq 1 reveal that the cores of the two complexes approach maximal congruency when the $\bar{4}$ and twofold axes are nearly perpendicular. With $[Fe_4S_4(SCH_2Ph)_4]^{3-}$ as the reference and $[Fe_4S_4(SPh)_4]^{3-}$ as the image molecule there are four such orientations that are nearly equivalent[21] and these may be achieved with the structures in Figure 1 by the means described.[22] The structural differences between the two trianions stand in contrast to the near-perfect core congruencies of $[Fe_4S_4(SPh)_4]^{2-}$ and $[Fe_4S_4(SCH_2Ph)_4]^{2-}$.

C. $[Fe_4S_4(SCH_2Ph)_4]^{2-}$ vs. $[Fe_4S_4(SCH_2Ph)_4]^{3-}$. Taking the dianion Fe_4 group or its entire core as the reference and the trianion Fe_4 group or its entire core as the image, two virtually degenerate, maximally congruent orientations of image with reference were found in both sets of calculations. These require parallel reference $\bar{4}$ and image twofold axes of the cores and produce the *same* orientations of the Fe_4 groups separately or as part of their respective cores. Degenerate orientations arise from a rotation about the twofold axis. Maximally congruent dianion and trianion core orientations[23] are shown in Figure 1; structural parameters are compared in Table IX. The principal core structural differences found upon passing from dianion (D_{2d}) to trianion (C_{2v}) are changes in the numbers of long and short Fe-S* distances, increases in mean values of long and short Fe-S* bonds and S*···S* interactions (whose two-long/four-short pattern is preserved), and a significant volume expansion (5.1%) of the S_4* tetrahedra (compared to 1.5% for the Fe_4 tetrahedra). The larger size of the trianion core derives predominantly from its longer Fe-S* bonds, which can be traced to the increased Fe(II) core character.[7,19]

Environmental Effects on Structure. As already emphasized the compressed tetragonal geometry of $[Fe_4S_4*]^{2+}$ cores is essentially constant in proteins[12,13,20] and synthetic compounds.[8-11] As evidenced by the structure of $(Et_3MeN)_3[Fe_4S_4(SPh)_4]$[7] and $(Et_4N)_3[Fe_4S_4(SCH_2Ph)_4]$, this does not appear to be the case for $[Fe_4S_4*]^+$ cores. The structure of the latter compound currently provides the only example of nontetragonal core geometry in $Fd_{ox,red}$ synthetic analogues which has been determined by X-ray diffraction.[24] Differences between core structures in these two compounds are presumably due to crystalline environmental effects. In an attempt to locate these effects, the distances between all atoms of a trianion and its neighboring ions were carefully examined. No unusually close packing contacts were observed. However, inspection of the unit cell packing diagram in Figure 4 reveals that the trianion has a rather extended conformation in the crystal with the pair of benzyl groups on each core face extending outward and lying roughly parallel to the *a* axis of the unit cell. This extended conformation is also evident in the stereoview of the complex (Figure 3). The core is approached on four sides by cations while its other two faces are shielded by benzyl groups. This arrangement differs from the somewhat more isotropic counterion environment of the trianions in $(Et_3MeN)_3[Fe_4S_4(SPh)_4]$, as may be seen by comparison of Figure 4 with the packing diagram for that structure.[7]

The crystalline environmental differences of $[Fe_4S_4(SCH_2Ph)_4]^{3-}$ and $[Fe_4S_4(SPh)_4]^{3-}$ in the preceding compounds, while not interpretable in terms of the stabilization of a specific core structure, are considered the primary causative factor for the difference in these structures. In turn, core structural differences, although small, are proposed as the principal source of the variations in Mössbauer parameters and magnetic moments (μ_t) observed in the solid state (Table I). In addition, properties of $[Fe_4S_4(SCH_2Ph)_4]^{3-}$ in different crystalline salts vary. For example, μ_t (4.2 K) = 3.35 μ_B in the Et_4N^+ and 2.60 μ_B in the *n*-Pr_4N^+ salt with substantial differences continuing to $\sim$ 340 K.[7] In comparison, salts of $[Fe_4S_4(SPh)_4]^{3-}$ have μ_t (4.2 K) = 2.05 (Et_4N^+) and 2.03 μ_B (Et_3MeN^+), with smaller differences in moments at higher temperatures than for salts of the benzylthiolate trianion. These results further suggest that, of the two trianions, $[Fe_4S_4(SCH_2Ph)_4]^{3-}$ is the more prone to environmental perturbations in the solid state.

Structural Changes and Electron Transfer. The near coincidence of Mössbauer and magnetic properties of the two trianions in frozen acetonitrile solutions and of magnetic properties in fluid solution (Table I) is the basis for the previously offered interpretation[7] that, when released from the environ-

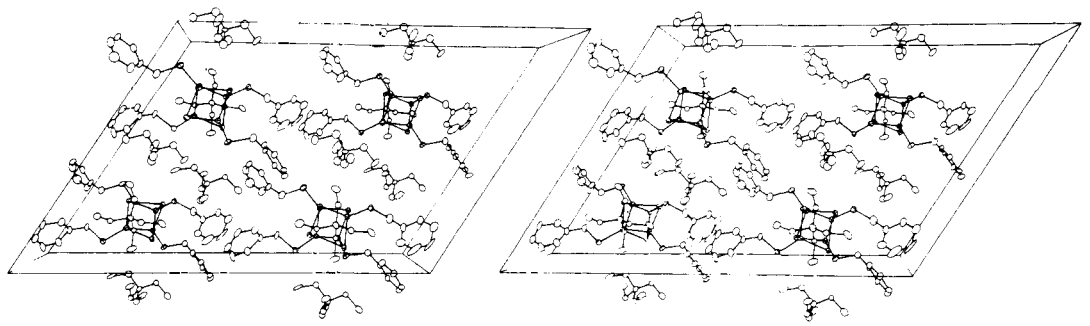

Figure 4. A stereoview of the unit cell of $(Et_4N)_3[Fe_4S_4(SCH_2Ph)_4]$; the a axis is horizontal, the c axis is vertical, and the view is down the b axis. Thermal ellipsoids are plotted at the 10% probability level; hydrogen atoms are omitted.

mental perturbations of a crystalline phase, $[Fe_4S_4(SCH_2Ph)_4]^{3-}$ approaches or achieves the elongated D_{2d} structure of $[Fe_4S_4(SPh)_4]^{3-}$. Assuming that extrinsic perturbing influences are much reduced in the solution vs. the solid state, the elongated tetragonal structure is the intrinsically stable form of the trianion oxidation level. Hence the *unconstrained* core structural changes pursuant to electron transfer in solution are considered to be those shown schematically in eq 2,[25] rather than a conversion between the D_{2d} and C_{2v} forms

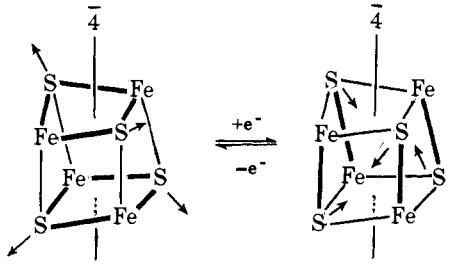

$[Fe_4S_4(SR)_4]^{2-}$ compressed D_{2d} $\quad$ $[Fe_4S_4(SR)_4]^{3-}$ elongated D_{2d} (2)

of $[Fe_4S_4(SCH_2Ph)_4]^{2-}$ and $[Fe_4S_4(SCH_2Ph)_4]^{3-}$, respectively, in Figure 1. Structural results indicate that the atoms of the S_4* group execute substantial movement with respect to the Fe_4 tetrahedron of similar but not identical dimensions in the two oxidation levels. Previous calculations[7] for $[Fe_4S_4(SPh)_4]^{2-,3-}$ have shown that the Fe_4 tetrahedra in the two oxidation levels are maximally congruent when their core 4 axes are parallel. With the Fe_4 unit as the more constant structural component of the core, the two oxidation levels can be interconverted by, primarily, the indicated S* atom displacements. This is an appealing physical picture for core structural changes in a protein where the Fe_4 group is bonded directly to the protein structure and is thus expected to maintain a nearly fixed orientation with respect to that structure. The maximally congruent orientations of the entire cores of $[Fe_4S_4(SPh)_4]^{2-,3-}$ place their $\bar{4}$ axes approximately perpendicular to each other. While these orientations[22] (Figure 1), as in previously considered cases, provide pictorially informative structural comparisons, there is obviously no necessity that electron transfer between spatially fixed cores will interconvert maximally congruent orientations of the entire core. The structural changes schematically depicted in eq 2 provide only a speculative picture for proteins until such time as the $[Fe_4S_4*]^{+}$ core structure in a Fd_{red} protein becomes defined. The proposition that protein structural factors could cause departures of the core of $[Fe_4S_4(S\text{-}Cys)_4]$ sites in Fd_{red} proteins from the inherently preferred elongated tetragonal geometry, and thereby affect redox potentials,[7] receives support from the now demonstrated sensitivity of the $[Fe_4S_4(SCH_2Ph)_4]^{3-}$ structure to environment.

The structural flexibility of additional $[Fe_4S_4(SR)_4]^{3-}$ complexes is under continuing investigation.[26] Results of EPR, Mössbauer, spectral, and magnetic susceptibility measurements indicate that in their crystalline states the trianions of $(Et_4N)_3[Fe_4S_4(SR)_4]$ (R = p-$C_6H_4CHMe_2$, CH_2-p-C_6H_4OMe) and $(Me_4N)_3[Fe_4S_4(SR)_4]$ (R = m-, p-C_6H_4Me) also depart from elongated tetragonal geometry, but revert to this configuration in frozen solutions. Evidently, nontetragonal core structures of $[Fe_4S_4(SR)_4]^{3-}$ species in the solid state, unlike the case of $[Fe_4S_4(SR)_4]^{2-}$ complexes, are not an exceptional occurrence. Among other tetranuclear complexes, the closest parallel with the results described here and elsewhere[7] is found with a series of Cu(II) chelate species containing Cu_4O_4 cores with different arrangements of long Cu–O bonds.[27] Solid-state magnetic properties of structurally different forms of the same molecule are in some cases quite distinct.[28]

Acknowledgments. This research was supported by NIH Grant GM-22352. We thank Dr. M. A. Bobrik for early X-ray diffraction experiments, Dr. J. Renaud for crystal-growing experiments, Dr. K. N. Raymond for use of his diffractometer, and Dr. J. A. Ibers for supplying a computer program and for useful discussions and structure refinement calculations.

Supplementary Material Available: Values of F_o^2 and F_c^2 for $(Et_4N)_3[Fe_4S_4(SCH_2Ph)_4]$ (Table VII); calculated hydrogen atom positions (cations and anion, Table VIII) (19 pages). Ordering information is given on any current masthead page.

References and Notes

(1) Alfred P. Sloan Foundation Fellow, 1976–1978.
(2) R. H. Holm and J. A. Ibers in "Iron-Sulfur Proteins", Vol. III, W. Lovenberg, Ed., Academic Press, New York, 1977, Chapter 7.
(3) G. Palmer in "The Enzymes", Vol. XII, Part B, 3rd ed., P. D. Boyer, Ed., Academic Press, New York, 1975, pp 1–56.
(4) J. Cambray, R. W. Lane, A. G. Wedd, R. W. Johnson, and R. H. Holm, *Inorg. Chem.*, **16**, 2565 (1977).
(5) J. G. Reynolds, E. J. Laskowski, and R. H. Holm, *J. Am. Chem. Soc.*, **100**, 5315 (1978).
(6) R. W. Lane, A. G. Wedd, W. O. Gillum, E. J. Laskowski, R. H. Holm, R. B. Frankel, and G. C. Papaefthymiou, *J. Am. Chem. Soc.*, **99**, 2350 (1977).
(7) E. J. Laskowski, R. B. Frankel, W. O. Gillum, G. C. Papaefthymiou, J. Renaud, J. A. Ibers, and R. H. Holm, *J. Am. Chem. Soc.*, **100**, 5322 (1978).
(8) B. A. Averill, T. Herskovitz, R. H. Holm, and J. A. Ibers, *J. Am. Chem. Soc.*, **95**, 3523 (1973).
(9) L. Que, Jr., M. A. Bobrik, J. A. Ibers, and R. H. Holm, *J. Am. Chem. Soc.*, **96**, 4168 (1974).
(10) H. L. Carrell, J. P. Glusker, R. Job, and T. C. Bruice, *J. Am. Chem. Soc.*, **99**, 3683 (1977).
(11) M. A. Bobrik, K. O. Hodgson, and R. H. Holm, *Inorg. Chem.*, **16**, 1851 (1977).
(12) E. T. Adman, L. C. Sieker, and L. H. Jensen, *J. Biol. Chem.*, **248**, 3987 (1973); **251**, 3801 (1976).
(13) C. W. Carter, Jr., in ref 2, Chapter 6.
(14) M. A. Bobrik, E. J. Laskowski, R. W. Johnson, W. O. Gillum, J. M. Berg, K. O. Hodgson, and R. H. Holm, *Inorg. Chem.*, **17**, 1402 (1978).
(15) In addition to the local data reduction program ENXDR and MULTAN, the programs used included full-matrix least-squares and Fourier programs; ABSCOR, a numerical method absorption correction program which applies a Gaussian grid to the crystal; CHORT, a numerical decay correction program; a modified version of ORFFE (Busing and Levy's function and error program); and Johnson's ORTEP. All calculations were carried out on a PDP 11/55 computer. Atomic scattering factors were taken from "International Tables for X-ray Crystallography", Vol. IV, Kynoch Press, Birmingham, England, 1974.
(16) See paragraph at end of paper regarding supplementary material.

(17) This program was written by J. A. Ibers.
(18) (a) $[Cp_4Fe_4S_4]^z$: z = 0, R. A. Schunn, C. J. Fritchie, Jr., and C. T. Prewitt, *Inorg. Chem.*, **5**, 892 (1966); C.-H. Wei, G. R. Wilkes, P. M. Treichel, and L. F. Dahl, *ibid.*, **5**, 900 (1966). z = 1+, Trinh-Toan, W. P. Fehlhammer, and L. F. Dahl, *J. Am. Chem. Soc.*, **99**, 402 (1977). z = 2+, Trinh-Toan, B. K. Teo, J. A. Ferguson, T. J. Meyer, and L. F. Dahl, *ibid.*, **99**, 408 (1977). (b) $Fe_4S_4(NO)_4$: R. S. Gall, C. T.-W. Chu, and L. F. Dahl, *ibid.*, **96**, 4019 (1974). (c) $[Fe_4S_4(S_2C_2(CF_3)_2)_4]^{2-}$: I. Bernal, B. R. Davis, M. L. Good, and S. Chandra, *J. Coord. Chem.*, **2**, 61 (1972). (d) $[Re_4S_4(CN)_{12}]^{4-}$: M. Laing, P. M. Kiernan, and W. P. Griffith, *J. Chem. Soc., Chem. Commun.*, 221 (1977).
(19) For high-spin $Fe^{II,III}$–SR distances cf. (a) R. W. Lane, J. A. Ibers, R. B. Frankel, G. C. Papaefthymiou, and R. H. Holm, *J. Am. Chem. Soc.*, **99**, 84 (1977); (b) D. Coucouvanis, D. Swenson, N. C. Baenziger, D. G. Holah, A. Kostikas, A. Simopoulos, and V. Petrouleas, *ibid.*, **98**, 5721 (1976).
(20) C. W. Carter, Jr., *J. Biol. Chem.*, **252**, 7802 (1977).
(21) For the four maximally congruent orientations the following deviations in distances between proximal vertices of the two core polyhedra were found: Fe···Fe, 0.028, 0.035, 0.009, 0.023 Å (mean 0.024 Å); S*···S*, 0.048, 0.032, 0.057, 0.032 Å (mean 0.042 Å).
(22) The display in Figure 1 of maximally congruent dianion–trianion core orientations precludes presentation of maximally congruent trianion–trianion orientations without recourse to additional structural depictions (not shown).
(23) For these orientations the following information corresponding to that in footnote 21 was obtained: Fe···Fe, 0.044, 0.036, 0.050, 0.022 Å (mean 0.038 Å); S*···S*, 0.057, 0.024, 0.042, 0.034 Å (mean 0.039 Å).
(24) To ensure that there were no systematic errors in the methods applied to the solution and refinement of the structure reported herein, a second data set was collected on a second crystal of similar size using an Enraf-Nonius CAD4 diffractometer and Mo $K\bar{\alpha}$ radiation. The data were processed as described in the Experimental Section and the structure was refined to convergence using the parameters reported in Table III as starting values. A comparison of the final set of coordinates with the data of Table III revealed no deviations greater than about 3σ for the anions, with deviations of the core atom coordinates averaging less than 1σ. A comparison of the 12 Fe–S bond distances of the core refined from the two different data sets revealed a mean difference of 0.003 Å (while the average error in a single Fe–S bond distance as estimated from the variance-covariance of the least squares was 0.005 Å). The greatest difference in Fe–S distances observed was 0.008 Å. To further ensure that there were no significant systematic errors in the refinement procedure, a second refinement was carried out on the CAD4 data set using the NUCLS program of Ibers. In this refinement the phenyl ring carbon atoms of the anions were treated as rigid groups with each atom in the group having its own isotropic temperature factor. The methylene carbons of the benzyl groups were also refined anisotropically. Inspection of the positions for the 12 core atoms from each of the refinements of this second data set revealed an average difference in fractional cell coordinates of 0.000 31 with least-squares estimated errors of 0.0003. In terms of distances, the average difference for the 12 Fe–S bonds was 0.0038 Å with the average estimated error of an individual distance being 0.005 Å. The largest difference observed was 0.011 Å. The two data sets, refined to give three separate sets of coordinates, all resulted in essentially the same core structure for the $[Fe_4S_4(SCH_2Ph)_4]^{3-}$ anion. The greatest difference among the core atomic coordinates of any of the three sets was 3.4σ and the greatest difference in any Fe–S bond distance was 0.019 Å. The average coordinate and Fe–S distance differences between any set were about 1σ. These results conclusively eliminate systematic errors in data collection, processing, and refinement as being responsible for the observed nontetragonal core distortion for the structure of $[Fe_4S_4(SCH_2Ph)_4]^{3-}$.
(25) This process is described more fully elsewhere.[7]
(26) E. J. Laskowski, J. G. Reynolds, R. B. Frankel, S. Foner, G. C. Papaefthymiou, and R. H. Holm, results to be published.
(27) J. A. Bertrand and J. A. Kelley, *Inorg. Chim. Acta*, **4**, 203 (1970); R. Mergehenn, L. Merz, W. Haase, and R. Allman, *Acta Crystallogr., Sect. B*, **32**, 505 (1976); R. Mergehenn and W. Haase, *ibid.*, **33**, 1877 (1977), and references cited therein.
(28) L. Merz and W. Haase, *Z. Naturforsch. A*, **31**, 177 (1976); L. Merz, W. Haase, and G. Keller, *Ber. Bunsenges. Phys. Chem.*, **80**, 305 (1976).

Studies on Vitamin B_{12} and Related Compounds. 49. Direct Synthesis of Alkyl- and of ω-Carboxyalkylcobalamins from Vitamin B_{12} and Aliphatic Carboxylic Acids under "Oxidizing–Reducing" Conditions[1]

Gerhard N. Schrauzer* and Masao Hashimoto[2]

Contribution from the Department of Chemistry, University of California at San Diego, Revelle College, La Jolla, California 92093. *Received September 22, 1978*

Abstract: Straight-chain aliphatic carboxylic acids $C_nH_{2n+1}COOH$ (n =, e.g., 1–6) and certain dicarboxylic as well as branched carboxylic acids can be oxidized to organic radicals in the presence of vitamin B_{12r} and converted into organocobalamins. Owing to the instability of secondary and tertiary alkylcobalamins and other steric effects, vitamin B_{12r} acts as a selective scavenger of primary alkyl and ω-carboxyalkyl radicals. Accordingly, *n*-alkylcobalamins and ω-carboxyalkylcobalamins are isolated exclusively and often in quantitative yields. The alkyl and carboxyalkyl radicals are generated from the carboxylic acids by $HO_2\cdot$, $O_2^-\cdot$, or HO· radicals formed in reactions of limiting amounts of O_2 preferably with V(III) salts, although V(IV), Mo(III), and certain other reducing metal ions can also be used. Oxygen can furthermore be replaced by H_2O_2, by Fenton reagent, or by electrochemically generated oxygen or oxygen radicals. The reducing metal ions, e.g., V(III), must be present in excess. They not only act as activators of oxygen, but also as reductants of vitamin B_{12}, thus maintaining it in the reactive Co(II) state. The new method of synthesis of organocobalamins under "oxidizing–reducing" conditions may become useful for the preparation of otherwise difficultly accessible compounds.

The starting point of the present study was the observation that *methylcobalamin* (**1**) and *carboxymethylcobalamin* (**2**)[3]

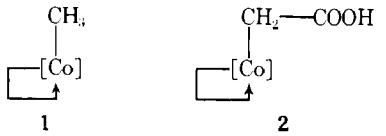

1 **2**

were formed in a reaction in which acetate-buffered solutions of vitamin B_{12r} were reacted with limiting amounts of oxygen in the presence of V^{3+}(aq) ions.

The question of how methylcobalamin could be synthesized from acetic acid and vitamin B_{12} under nonenzymatic conditions has intrigued the senior author for many years, following the report that this reaction occurs, either directly or indirectly, in cells or cell extracts of the methanogenic bacterium *Methanosarcina barkeri*.[4] Assuming that this reaction occurs directly, many unsuccessful attempts were made in our laboratory to verify this reaction under nonenzymatic conditions, suggesting that a specific activation of acetate was necessary or that the transfer occurred indirectly. The new observation indicated that **1** can be formed from acetate by way of an ox-

0002-7863/79/1501-4593$01.00/0